

SPRING DRINKING WATER OPTICAL PROPERTIES (420nm-700nm) IN HILLY REGION NEAR NISI KHOLA AREA BAGLUNG, NEPAL

^{1,3,4}Saddam Husain Dhobi, ^{1,4}Uday Khatri, ^{1,4}Kishori Yadav, ^{2,4}Kuldip Paudel, ^{1,4}Bibek Koirala, ^{1,4}Jeevan Jyoti Nakarmi, ^{1,3,4}Rina Waiba, ^{1,4}Amrit Nepali

¹Department of Physics, Patan Multiple Campus, Tribhuvan University, Lalitpur-44700, Nepal

²Department of Physics, St. Xavier's College, Tribhuvan University, Kathmandu-44600, Nepal

³Robotics Academy of Nepal, Lalitpur-44700, Nepal

⁴Innovative Ghar Nepal, Lalitpur-44700, Nepal

Email: saddam@ran.edu.np

Abstract

To measure the transmittance of drinking water, 2W LED light, Theremion Spectrometer and diffraction grating are used. The research area is Nisi located in Baglung district, Nepal. The observation is taken 9 sample of drinking water taken from different sources of Nisi. The observation shows that the transmittance of drinking water taken from Kanabazer, Jiba Khola, Jiri, Jajir, Khahare Khola, Bhalu Khola and Nisi Khola is high. In addition, the absorbance of drinking water taken from Khar Chowar is higher than other. The transmittance of the sample ranges from 32% to 100% while absorption coefficient $0.034 \times 10^2 m^{-1}$ to $1.110 \times 10^2 m^{-1}$. The coefficient of determination ranges of samples from 0.771 to 0.983 and standard deviation ranges from 0.0075 to 0.0807.

Key Words: - Absorbance, Diffraction Grating, Drinking water, Nisi Khola, Theremion Spectrometer, Transmittance

1. Introduction

The presence of organic chemicals and their identification using photonic technology is one of the most difficult challenges, and the possibility of removing them by identifying them is now under investigation. Because organic compounds are harmful to humans when consumed [1]. Natural and human-caused water contamination is a major environmental and health hazard. Insecticides and pesticides, heavy metals and sewage, medications and personal care items are among the human pollutants. Chromatography, electrode potentiometry, mass spectrometry, UV-Vis spectroscopy, and Raman scattering are some of the technologies used to detect contaminants in water. The use of resistivity, temperature, pH, total suspended solids (TSS), UV-254 absorbance, and total organic content for dispersed and continuous water quality monitoring is gaining popularity (TOC). In the range 250 nm to 350 nm, pure water has a scattering-independent absorption coefficient of less than $0.1 m^{-1}$, with a minimum of less than $10^{-3} m^{-1}$ at the top end of this range [2].

According to Singh and Pandey, the world's urban population is predicted to increase to 68% by 2050, with repercussions for Himalayan regions as well. Water governance in such locations remains a blind spot, with difficulties related to urban water resilience being poorly recognized. Kumar et al. (1997) investigated the physico-chemical properties of water from 12 springs within the municipal limits of Almora, a Himalayan town in central India [3]. According to Merz et al. (2004), a female member of the home fetches water in 79% of the questioned

families in the Jhikhu Khola. Many residents in the watershed's upper reaches rely on natural springs for their water [4]. Siwalik zone heights range from 900 to 1200 meters, with an area of 8%. South of the middle mountain is Siwalik zone. The Middle Hills range in elevation from 1200 to 3000 meters, with a 30% area. With an area of 20%, the High Mountains are at an elevation of 3000-5000m. Nepal has a high Himalayan height of >5000m and a 9% Himalayan land.

Stream water sources are one of the main water sources in Bahun Khola. During the dry season, the creek totally dries up, since any accessible water is gathered for home water supply. During the dry season, there is insufficient water for irrigation, therefore they re-use domestic water. Water consumption has remained relatively stable over the last five years, although increased population has resulted in higher consumption. The main water supply source in the Baad Khola area is groundwater seepages and springs. In addition, irrigation uses a modest amount of water. During the post-monsoon season, flow in the stream downstream of the spring source was estimated to be 10 l/s [5]. Millions of people around the world, particularly in rural regions, still lack access to safe drinking water, sanitation, and basic hygiene services, despite the global goal of universal access by 2030. In the world, 44% of all wastewater flows generated by households are not treated safely. Although the ambient water quality of 60% of the world's monitored water bodies is good. Rapid changes in the area covered by surface waters are occurring in one-fifth of the world's river basins, indicating flooding and drought events linked to climate change. Despite growing financing needs to reach SDG targets, official development aid (ODA) commitments to the

water sector have remained constant in recent years. In 2020, over 2 billion people, or 26% of the world's population, lacked access to safe drinking water on their premises, which was available when needed and free of contamination [6].

Clean water scarcity is a big concern in today's globe of 7.7 billion people, according to the United Nations and the World Water Development Report. By 2050, the world population will have risen by 22 to 34 % to 9.4 to 10.2 billion people, putting a pressure on the water infrastructure. Currently, little less than half of the world's population, 3.6 billion people (47%) live in locations where water scarcity occurs at least once a year. More than half of the world's population (57%) will live in locations where water scarcity occurs at least once a year by 2050. Currently, 12% of the world's population drinks water from unimproved and potentially dangerous sources. More than a third of the world's population, or 2.4 billion people, lack access to sanitation. In underdeveloped countries, 90% of sewage is dumped into the water untreated. 730 million tons of sewage and other effluents are dumped into the water every year.

Every year, industry releases 300 to 400 megatons of garbage into the sea. The degradation of fresh-water habitats owing to pollution of water resources and aquatic ecosystems has resulted in the loss of more than 30% of global biodiversity. In agriculture, wastewater recycling is crucial for livelihoods, but it also poses major health problems. Water contamination has gotten worse during the previous three decades, affecting practically every river in Africa, Asia, and Latin America. Currently, 80% of industrial and municipal wastewaters are discharged without treatment. By 2050, global fertilizer consumption is expected to rise from roughly 90 million tons to more than 150 million tons. By 2050, phosphorus and nitrogen effluents will have increased by 180 % and 150 %, respectively. Herbicides account for 47.5 % of all chemicals used in agriculture, with insecticides accounting for 29.5 %, fungicides for 17.5 %, and miscellaneous chemicals accounting for 5.5 %. In summary, by 2050, the demand for water will increase while the supply of water will decrease [7].

From around 10,000 to 5000 BC, the entire global population remained relatively stable, accounting for less than five million individuals. It began to increase during the Bronze Age, reaching a peak of 50 million people by the end of the period, and peaked at around 190 million in the year 200 AD. The rise was moderate in the following years, with 265 million in 1000 AD and 350 million in 1400 AD. The global population rose steadily after 1500 AD, reaching one billion people 200 years ago. However, the increase was significant between 1900 and 2000, going from 1.5 to 6.1 billion in just 100 years and, most impressively, from

2.50 billion in 1950 to 7.55 billion today [8]. According to the World Health Organization (WHO, 2019), 2.6 billion people lack basic sanitation, and 1.8 million people die each year as a result of water-related diseases. Diarrheal illnesses claimed the lives of 499,000 children under the age of five in 2015, accounting for 8.6% of all deaths in this age group [9].

Diarrhoea is one of Nepal's most common water-borne diseases, caused by poor sanitation, hygiene, and water quality. The frequency of diarrhoea among children under the age of five years was 131 per 1,000 children in 1995/96. The diarrhoea mortality rate was 0.34 per 1000 children under the age of five, while the fatality rate was 2.56 per 1,000. (CBS, 2001). Diarrhoea is becoming more common in Nepal at an alarming rate. According to a report from Kathmandu's Teku Hospital, water-borne sickness was responsible for 16.5 % of all deaths (Metcalf, 2000). *Salmonella typhi*, the organism that causes typhoid fever, and *Vibrio cholerae*, the organism that causes cholera (Madigan et al., 1997) [10] are probably the most important pathogenic bacteria transferred through water. Water supply and sanitation investments are principally driven by the government's Water Plan 2002–27, which aims to achieve universal coverage of basic water supply and sanitation by 2017. The Plan also aimed to upgrade 27 % of the population's basic water supply to a medium to high level by 2017, and 50 % by 2027. It has not, however, set goals for improving sanitary services [11].

2. Materials and Method

To study the absorbance and transmittance of water used experimental method. The experiment was taken by measuring the intensity of visible light using *Theremino_Spectrometer* software and diffracting grating. The experiment was on different 9 sample of drinking water sources from Baglung, around Nisi Khola Area, Nepal. The first sample (S1) is taken from Kanabazer, second sample (S2) from Jiba Khola, third sample (S3) from Jiri, fourth sample (S4) from Jajir, fifth sample (S5) from Khahare Khola, sixth sample (S6) from Khar Chowar, seventh sample (S7) from Bas Khola, eighth sample (S8) from Bhalu Khola and sample ninth (S9) from Nisi Khola drinking water sources. All samples sources of drinking water sources mixed on Nisi Khola which is consider as S9. It is necessary to study the absorbance and transmittance coefficient of drinking water around Nisi Khola because absorbance and transmittance help to understand the dissolved particle properties (organic, inorganic, total dissolve solute) in drinking water with interaction.

According to the block diagram in Fig.1, the source white LED emits white light that contains seven different visible colors as it passes through the drinking water. Some light is absorbed, while others are transmitted through the sample (represented by a thin blue arrowhead). The transmitted light

from the samples strikes the Theremino Spectrometer sensor, which generates data that is recorded/observed in a computer. Origin software was used to arrange and plot the recorded data. The experiment was carried out in a darkroom to avoid interference from outside sources, as these interfered with the intensity of incident light on the sample. Except for the temperature, the experiment for both samples is ideal.

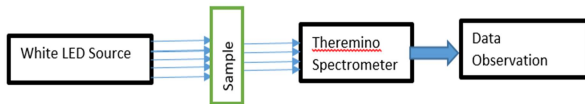


Figure 1: Block Diagram of an experiment to study the Transmittance and Absorption Coefficient of Sample

When compared to reverse osmosis, UV treatment, and Ozonations, etc., testing the purities of drinking water based on transmittance coefficient is simple, chemical-free, less expensive, and takes less time. A large number of contaminants are removed by pushing water under pressure through a semi-permeable membrane in reverse osmosis (RO) phenomena. RO does not provide any information about the transmittance coefficient or temperature for testing water purity. In the ozonization phenomenon, ozone is formed by dissociating molecular oxygen to form ozone, which is used to disinfect wastewater. However, this phenomenon does not provide any information about the transmittance coefficient or temperature for testing the purity of water.

UV water treatment is used to kill microorganisms in water but does not provide information on transmittance and temperature for testing water purity. To provide pure, healthy drinking water, sophisticated purification technology, also known as an advanced oxidation system or complex system, is used. In this phenomenon, Ozonization, RO, and other beneficial water purification systems are used to create pure drinkable water. This testing technique is cheaper without serious hazard during testing. The transmittance shows the TDS quantity present in water and absorbance shows the presence of optical properties of TDS. The absorption coefficient of samples are compare with pure water to study the optical properties of Nisi Khola drinking water. The research area in noted in Fig.2.

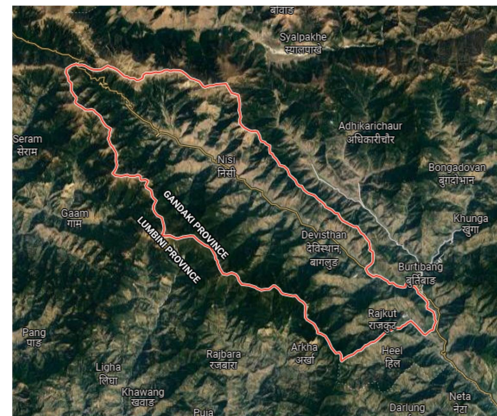


Figure 2: Research area Baglung, Nepal accessed at 11/19/2021

The absorbance A is defined as $\{2 - \log(T[\%])\}$ where transmittance of sample is defined as $T\% = \left(\frac{I}{I_0}\right) \times 100\%$ and I is intensity of light after passing through sample while I_0 is intensity of light before passing sample

3. Result and Discussion

3.1. Optical Properties of Baglung Water Samples, Nepal

Because of their increased turbidity, Prieto et al. (2020) showed that lower water transmittance indicates more pollutant in samples. They used wavelength (380-700 nm) to assess transmittance and absorbance and discovered that the nature of the graph is steeper with varied slop with wavelength. The change in slope is due to the interaction of organic matter with light because organic matter absorbs more energy at low wavelengths (UV near-visible range), although visible transmission is highest in comparison to UV [12]. In the visible range of light, the nature obtained by Prieto et al. is comparable to that obtained by Feret et al. (2008), Buiteveld et al. (1994), Kout et al. (1993), Wieliezka et al. (1989) for pure water [13]. Pegau et al (1997) [14] also established the nature with steeper and slope with wavelength for clean water. The absorption coefficient was calculated using $2.303A/cm$, where A is the absorbance and $T[\%]$ is an experimentally determined value.

The nature of absorption and transmittance of the sample obtained from different 9 sources of drinking water from Baglung, Nepal is similar to [12-14] as shown in Fig.3 but due to contamination present in water the value of transmittance and absorbance is different. The comparison are tabulated in table 1.

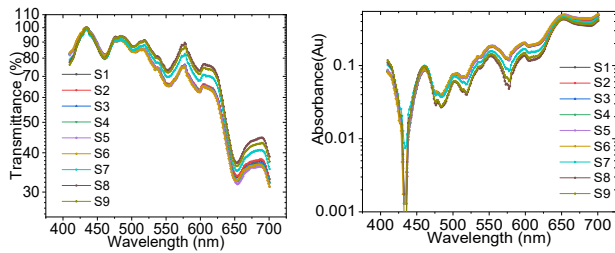


Figure 3: Transmittance and Absorbance of drinking water sources Baglung, Nepal

The shape of the water absorption spectrum in the visible wavelength range (Fig.3, right-side) is characteristics as in between 400-700 nm wavelength range absorption is low. The absorption at different is due to impurities/contaminated. The absorption increases with increasing wavelength and has shoulders at 475nm, 525nm and a small one at 660 nm. From 690 nm absorption increases rapidly until approximately 740 nm [17].

3.2. Maximum and Minimum Transmittance of Spectrum at certain fixed wavelength

Fig.4 generalized, to study the maximum and minimum transmittance of 9 samples. The minimum transmittance at 460.0nm was obtained in S7, S8 and S9. Similarly at 506.3nm in S3, at 554.6nm in S3, at 600nm in S5, at 652.5nm in S5. The detail visualized in shown in Fig.4 (right). The maximum transmittance at 434nm was obtained in S1, S2, S3, S4, S8 is 100%. Similarly at 483.6nm in S8 is 94%, at 517.7nm in S8 is 91.6%, at 605.7nm in S8 is 89.5%, at 689.4nm in S8. The detail visualized in shown in Fig.4 (right).

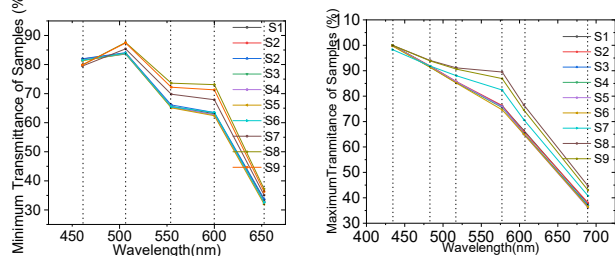


Figure 4: Minimum and Maximum transmittance at different wavelength of difference sample

3.3. Comparison of standard absorption coefficient of pure water with drinking water of present work

The absorption coefficient is high compare to [15-17] and present work. This is because the present work taken sample from natural source of drinking water (spring, spout, Sim: Nepali Name, etc.). The natural sources contain

different contaminated (organic, inorganic, TDS, mineral, etc.). Therefore due to presence of the contaminated in water the absorption high in compare to pure water as shown in table 1.

Table 1: Comparison of Absorption Coefficient of Drinking with Pure Water

| Wavelength (nm) | Absorption Coefficient (m^{-1}) | | | |
|-----------------|-------------------------------------|-------------------|-----------------------|------------------------|
| | Present work ($*10^2$) | Pope and Fry[15]. | Smith and Baker [16]. | Buiteveld et al. [17]. |
| 420 | 0.034-0.090 | 0.069 | 0.335 | 0.114 |
| 470 | 0.050-0.135 | 0.192 | 0.302 | 0.249 |
| 550 | 0.417-0.134 | 0.545 | 0.585 | 0.546 |
| 580 | 0.350-0.067 | 0.612 | 0.627 | 0.624 |
| 600 | 0.465-0.136 | 0.712 | 0.676 | 0.664 |
| 675 | 1.011-0.361 | 0.996 | 1.032 | 0.999 |
| 700 | 1.110-0.410 | 1.029 | 1.045 | 1.030 |

3.4. Statistical analysis of Samples

Fig.5, represent the best fitted graph for each samples with 95% confidence and prediction of every 9 samples of drinking water. The fitted equation for each samples is 9 degree polynomial equation. The fitted equation for S1 is represented by y_{S1} , S2 by y_{S2} , S3 by y_{S3} , S4 by y_{S4} , S5 by y_{S5} , S6 by y_{S6} , S7 by y_{S7} and S9 by y_{S9} . Here y represent the absorbance and the term variable x represent wavelengths of light. The term without x in equation represent the intercept.

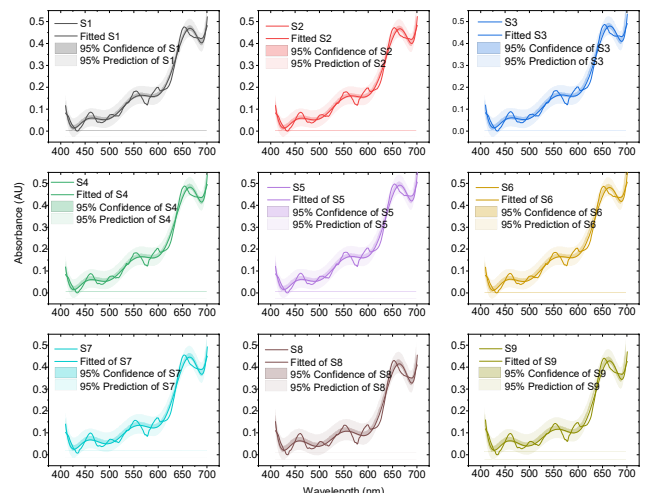


Figure 5: Best fit with 95% confidence and prediction of different samples

The polynomial equation of 9 degree for each samples are given below;

$$y_{S1} = 91289.10 + 1927.15x - 17.27x^2 + 0.09x^3 - 2.77 \times 10^{-4}x^4 + 5.74 \times 10^{-7}x^5 - 7.78 \times 10^{-10}x^6 + 6.69 \times 10^{-13}x^7 - 3.31 \times 10^{-16}x^8 + 7.20 \times 10^{-20}x^9 \quad (1)$$

$$y_{S2} = -133635.59 + 2590.18x - 21.84x^2 + 0.11x^3 - 3.23 \times 10^{-4}x^4 + 6.50 \times 10^{-7}x^5 - 8.62 \times 10^{-10}x^6 + 7.27 \times 10^{-13}x^7 - 3.54 \times 10^{-16}x^8 + 7.59 \times 10^{-20}x^9 \quad (2)$$

$$y_{S3} = -131888.69 + 2562.06x - 21.64x^2 + 0.10x^3 - 3.21 \times 10^{-4}x^4 + 6.47 \times 10^{-7}x^5 - 8.58 \times 10^{-10}x^6 + 7.25 \times 10^{-13}x^7 - 3.53 \times 10^{-16}x^8 + 7.58 \times 10^{-20}x^9 \quad (3)$$

$$y_{S4} = -137137.75 + 2657.83x - 22.41x^2 + 0.11x^3 - 3.32 \times 10^{-4}x^4 + 6.67 \times 10^{-7}x^5 - 8.85 \times 10^{-10}x^6 + 7.47 \times 10^{-13}x^7 - 3.64 \times 10^{-16}x^8 + 7.80 \times 10^{-20}x^9 \quad (4)$$

$$y_{S5} = -143863.14 + 2768.51x - 23.22x^2 + 0.11x^3 - 3.41 \times 10^{-4}x^4 + 6.84 \times 10^{-7}x^5 - 9.05 \times 10^{-10}x^6 + 7.61 \times 10^{-13}x^7 - 3.70 \times 10^{-16}x^8 + 7.93 \times 10^{-20}x^9 \quad (5)$$

$$y_{S6} = -168470.68 + 3194.89x - 26.49x^2 + 0.13x^3 - 3.82 \times 10^{-4}x^4 + 7.62 \times 10^{-7}x^5 - 1.00 \times 10^{-9}x^6 + 8.40 \times 10^{-13}x^7 - 4.07 \times 10^{-16}x^8 + 8.67 \times 10^{-20}x^9 \quad (6)$$

$$y_{S7} = -19389.60 + 682.16x - 7.75x^2 + 0.05x^3 - 1.57 \times 10^{-4}x^4 + 3.48 \times 10^{-7}x^5 - 4.98 \times 10^{-10}x^6 + 4.45 \times 10^{-13}x^7 - 2.28 \times 10^{-16}x^8 + 5.09 \times 10^{-20}x^9 \quad (7)$$

$$y_{S8} = -66691.89 + 1510.40x - 14.15x^2 + 0.07x^3 - 2.39 \times 10^{-4}x^4 + 5.04 \times 10^{-7}x^5 - 6.94 \times 10^{-10}x^6 + 6.03 \times 10^{-13}x^7 - 3.01 \times 10^{-16}x^8 + 6.60 \times 10^{-20}x^9 \quad (8)$$

$$y_{S9} = -91289.08 + 1927.15x - 17.27x^2 + 0.09x^3 - 2.77 \times 10^{-4}x^4 + 5.74 \times 10^{-7}x^5 - 7.78 \times 10^{-10}x^6 + 6.69 \times 10^{-13}x^7 - 3.31 \times 10^{-16}x^8 + 7.20 \times 10^{-20}x^9 \quad (9)$$

3.5. R-Square (COD) for samples

The calculated R-square is observed above 0.935 by junior et al. (2019) for pure water for different samples [18] and in our study the value of R-square was found above 0.982 as shown in table 2.

This shows that there is correlation between wavelength and absorbance coefficient and equation (1) to (9) represented the ideal equation for each samples.

Table 2: Coefficient of determination for drinking water samples

| Sample | R ² | Adj.R-Sq. |
|--------|----------------|-----------|
| S1 | 0.975 | 0.974 |
| S2 | 0.982 | 0.981 |
| S3 | 0.983 | 0.982 |
| S4 | 0.982 | 0.981 |
| S5 | 0.983 | 0.982 |
| S6 | 0.982 | 0.981 |
| S7 | 0.983 | 0.982 |
| S8 | 0.968 | 0.966 |
| S9 | 0.971 | 0.969 |

Table3: Standard deviation at for all sample at common wavelength

| Wavelength (nm) | Absorption Coefficient (*10 ² m ⁻¹) of Samples | | | | | | | | | Standard Deviation |
|-----------------|---|-------|-------|-------|-------|-------|-------|-------|-------|--------------------|
| | S1 | S2 | S3 | S4 | S5 | S6 | S7 | S8 | S9 | |
| 420 | 0.104 | 0.104 | 0.109 | 0.120 | 0.114 | 0.095 | 0.144 | 0.137 | 0.124 | 0.0161 |
| 470 | 0.134 | 0.131 | 0.132 | 0.135 | 0.135 | 0.122 | 0.135 | 0.115 | 0.121 | 0.0075 |
| 550 | 0.414 | 0.408 | 0.419 | 0.417 | 0.423 | 0.423 | 0.355 | 0.309 | 0.322 | 0.0461 |
| 580 | 0.316 | 0.306 | 0.322 | 0.324 | 0.323 | 0.350 | 0.232 | 0.154 | 0.179 | 0.0714 |
| 600 | 0.461 | 0.454 | 0.465 | 0.467 | 0.472 | 0.454 | 0.387 | 0.313 | 0.338 | 0.0613 |
| 700 | 1.109 | 1.110 | 1.130 | 1.140 | 1.165 | 1.165 | 1.036 | 0.944 | 0.981 | 0.0807 |

4. Conclusion

On observing the transmittance and absorbance of drinking water source from Baglung, Nepal from different places. It

is found that that minimum transmittance is 32% at 652.5nm for sample 8. The maximum transmittance is observed is 100% for sample 1, sample 2, sample 3, sample 4, sample 5, sample 8 and sample 9. The absorbance coefficient at 420nm is $0.034 \times 10^2 m^{-1}$ while at 700nm is $1.110 \times 10^2 m^{-1}$. The coefficient of determination ranges of samples from 0.771 to 0.983 and standard deviation ranges from 0.0075 to 0.0807.

Acknowledgments

Authors would like to thanks all the members of Department of Physics, Patan Multiple Campus, Tribhuvan University; Innovative Ghar Nepal, Robotics Academy of Nepal, Lalitpur-44700, Nepal for Providing experimental material and setup during research time.

References

- [1] S. Szerzyna, M. Mołczan, M. Wolska, W. Adamski, and J. Wiśniewski, "Absorbance based water quality indicators as parameters for treatment process control with respect to organic substance removal," E3S Web Conf. **17**(00091), 1-2 (2017).
- [2] M. Spangenberg, J. I. Bryant, S.J. Gibson, P. J. Mousley, Y. Ramachers, and G. R. Bell, "Ultraviolet absorption of contaminants in water," Sci. Rep. **11**(3682), 1-3 (2021).
- [3] A. Prakash, and D. Molden, "Editorial Mapping challenges for adaptive water management in Himalayan towns," IWA Publishing Alliance House, UK, 1-2 (2020).
- [4] J. Merz, G. Nakarmi, S. Shrestha, B.M. Dahal , B. S. Dongol, M. Schaffner, S. Shakya, S. Sharma, and R. Weingartner, "Public Water Sources in Rural Watersheds of Nepal's Middle Mountains: Issues and Constraints," Environ. Manage. **34**(1), 26–37, (2004).
- [5] S. H. Bricker, S. K. Yadav, A. M. MacDonald, Y. Satyal, A. Dixit, and R. Bell, "Groundwater resilience Nepal: Preliminary findings from a case study in the Middle Hills," British Geological Survey, Groundwater Science Programme, Open Report, 1-40 (2014).
- [6] UN-Water, "Summary Progress Update 2021–SDG6–Water and Sanitation for all," Geneva, Switzerland, 1-10 (July 2021).
- [7] A. Boretta, and Lorenzo Rosa, "Reassessing the projections of the World Water Development Report," NPJ Clean Water, **2**(15), 1-5(2019).
- [8] UN, "World Population Prospects: The 2017 Revision," https://esa.un.org/unpd/wpp/Publications/Files/WPP2017_KeyFindings.pdf (accessed on 8 March 2021).
- [9] A. Lambert, S. Trow, C. Merks, B. Charalambous, A. Donnelly, S. Galea, M. Fantozzi, A. Hulsmann, J. Koelbl, J. Kovac, "EU Reference Document Good Practices on Leakage Management," WFD CIS WG PoM; European Commission: Brussels, Belgium, (2015).
- [10] T. Prasai, B. Lekhak, D. R. Joshi, and M. P. Baral, Microbiological Analysis of Drinking Water of Kathmandu Valley, Scientific World, **5**(5), 112-113(2007).
- [11] Government of Nepal, "National Water Supply and Sanitation Sector Policy 2014," Ministry of Urban Development. https://www.humanitarianresponse.info/sites/www.humanitarianresponse.info/files/documents/files/eng_wss_policy_2014_dr_aft-1.pdf (accessed on 23 October 2021).
- [12] D. C. Prieto, J. T. García, F. C. Cartagena, and J. S. Muro, "Wastewater Quality Estimation through Spectrophotometry-Based Statistical Models," Sensors, **20**(5631), 1-2 (2020).
- [13] S. L. Ustin, and S. Jacquemoud, "Chapter 14 How the Optical Properties of Leaves Modify the Absorption and Scattering of Energy and Enhance Leaf Functionality," Remote Sensing of Plant Biodiversity: Springer Nature, Switzerland, 349-377 (2020). <https://doi.org/10.1007/978-3-030-33157-3>
- [14] W. S. Pegau, D. Gray, and J. R. V. Zaneveld, "Absorption and attenuation of visible and near-infrared light in water: dependence on temperature and salinity," Appl. Opt. **36**, 6035-6045 (1997).
- [15] R. M. Pope, and E. S. Fry, "Absorption spectrum ~380–700 nm! of pure water. II. Integrating cavity measurements," Appl. Opt. **36**, 8710-8719 (1997).
- [16] R. C. Smith, and K. S. Baker, "Optical properties of the clearest natural waters ~200–800 nm," Appl. Opt. **20**, 177–184 (1981).
- [17] H. Buiteveld, J. H. M. Hakvoort, and M. Donze, "The optical properties of pure water," in Ocean Optics XII, J. S. Jaffe, ed., Proc. SPIE **2258**, 174–183 (1994).
- [18] R. A. M. Junior, G. S. Munhoz, and M. H. F. Medeiros, "Correlations between water absorption, electrical resistivity and compressive strength of concrete with different contents of pozzolan," Revista de la Asociación Latinoamericana de Control de Calidad, Patología y Recuperación de la Construcción, **9**(2), 2-4 (2019).